Motion Primitives for Human-Inspired Bipedal Robotic Locomotion: Walking and Stair Climbing

Matthew J. Powell, Huihua Zhao, and Aaron D. Ames

***Abstract*— This paper presents an approach to the development of bipedal robotic control techniques for multiple locomotion behaviors. Insight into the fundamental behaviors of human locomotion is obtained through the examination of experimental human data for walking on flat ground, upstairs and downstairs. Specifically, it is shown that certain outputs of the human, independent of locomotion terrain, can be characterized by a single function, termed the *extended canonical human function*. Optimized functions of this form are tracked via feedback linearization in simulations of a planar robotic biped walking on flat ground, upstairs and downstairs — these three modes of locomotion are termed "motion primitives." A second optimization is presented, which yields controllers that evolve the robot from one motion primitive to another — these modes of locomotion are termed "motion transitions." A final simulation is given, which shows the controlled evolution of a robotic biped as it transitions through each mode of locomotion over a pyramidal staircase.**

I. INTRODUCTION

The study of bipedal robotic locomotion has a rich history. An enormous variety of control approaches have been developed, including: passivity control [1], [2] and passive walkers [3], computation of zero-moment point [4], and clever use of compliance [5], [6], among others. Robotic stair-climbing has been achieved in [7], [8]. Bipedal robots are even now available [9] both commercially and for research. Impacts extend beyond the field with significant advances in prosthetic devices [10], [11], [12] and exoskeletons [13].

The quintessential model of bipedal locomotion — the human body — has an even richer history. Thousands of years of evolution has rendered the human locomotion system a highly effective, low-level control system. We suggest that examination of this system will yield unparalleled insight into the design of bipedal robotic locomotion controllers. Granted, the physical human system, which utilizes 57 muscles in locomotion [14], is far too complex to replicate with current hardware and computational capabilities; however, we claim that one can construct a low-level representation of the human locomotion system. That is, certain outputs of the human locomotion system can be represented as second order system responses.

This paper presents two main results; the first is an extension of [15], in which the author presents a method of automatically obtaining robotic walking controllers, via an optimization, from a set of human walking data. In the present paper, it is shown that an augmentation of the optimization can be successfully applied to multiple modes of locomotion. Specifically, the presented technique yields robot locomotion controllers for walking on flat ground, upstairs and downstairs. The second result is a method of obtaining controllers which evolve the robot from one locomotion mode to another; that is, controllers which yield transition modes between walking on flat ground, and traversing stairs. The combination of these two results is a collection of controllers, automatically obtained from optimizations about human data, which form a continuous, multi-modal system.

The study begins with examination of the human locomotion system. An experiment is performed, which yields human xyz-position data for flat ground walking, walking upstairs and walking downstairs; this data forms the foundation of our control approach. Using the method of [15], it is shown that certain outputs of the human data for flat ground walking, can be characterized by the response of a linear spring-damper system under constant force; this result is extended to accommodate walking upstairs and downstairs. Specifically, the *extended canonical human function* (2) is shown to represent sets of data, from all three modes of locomotion of interest, with high correlation in each case. The fact that the same function can be applied to different modes of locomotion further illustrates the validity of the proposed low-level representation of the human system.

A classification scheme for hybrid systems — the *meta-hybrid system* — is presented, in which a distinction is made between primary and auxiliary modes of locomotion, which are termed *motion primitives* and *motion transitions*, respectively. Motion primitives are fundamental modes of locomotion; the three motion primitives of this study are: walking on flat ground, walking upstairs and walking downstairs. To switch between different motion primitives in a stable manner, auxiliary modes, termed "motion transitions," are introduced.

Implementing the extended canonical function via feedback linearization, stable locomotion is achieved on a planar bipedal robot in simulations of each of the three motion primitives. Motion transitions are used to construct simulations which show the composition of multiple motion primitives together; that is, a simulation is given which shows the controlled evolution of a biped as it ascends and then descends a staircase.

II. HUMAN LOCOMOTION DATA

For guidance and insight in the control design process, we turn to the most prevalent source of information on bipedal

Department of Mechanical Engineering, Texas A&M University, College Station, TX 77843, e-mail: {mjpowell,huihuazhao,aames}@tamu.edu

The work of M. J. Powell is supported by NASA grant NNX11AN06H. The work of A. D. Ames is supported by NSF grant CNS-0953823.

walking found in nature — the human body. The following sections provide an overview of the analysis and the insights obtained through examination of the data.

A. Human Locomotion Experiments

A set of four human subjects participated in this study; each was outfitted with 19 LED sensors placed at key locations on the body, as illustrated in Fig. 2. As a test subject performed the desired task, data were collected from these sensors via the Phase Space Motion Capture System [16]. An experiment consisted of a single test subject performing three distinct modes of locomotion: walking on flat ground, ascending a stairway and descending a stairway. The stairway used in this experiment has a 0.25 meter stair height and a 0.27 meter stair depth. For this paper, we selected the subject whose data contained the least noise; and as we will discuss in the proceeding subsections, the analysis of these data forms the basis of our locomotion controller design.

Fig. 1: Human experiment for walking upstairs.

B. Automated Domain Breakdown

Here, the domain breakdown specifies the beginnings and ends of steps in human data. The domain breakdown is traditionally obtained via a position threshold which specifies when the heel is on the ground; however, we present an alternative method, which involves the examination of acceleration, rather than position, data to identify the specific times associated with maximum heel acceleration. The maximum heel accelerations occur prior to heel-ground impact and as the heel lifts.

This method is similar to the analysis of foot-ground forces, which is common in the biomechanics community [17], [18]. The general idea in these experiments is to collect force data from subjects walking on force-plate-forms, and then determine the domain breakdown through the periods of time in which the force on the plate is minimal. The advantage of using forces or accelerations, as opposed to position thresholds, is that the domain break down process is performed without user input, and thus, can be applied more readily to different sets of data.

The domain breakdown plays a critical role in the human-inspired locomotion controller design process; that is, the complete-step time intervals obtained through the domain breakdown specify the intervals of data over which our function fitting method is valid.

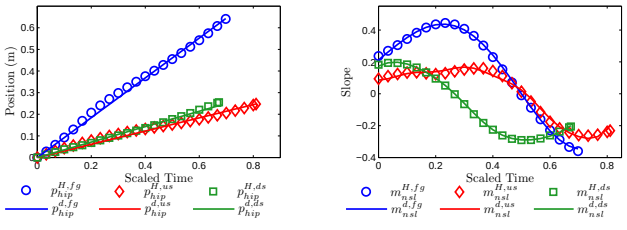

(a) Fitted hip position (b) Fitted nonstance slope

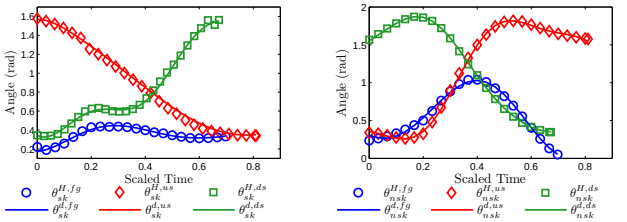

(c) Fitted stance knee angle (d) Fitted nonstance knee angle

Fig. 2: Fitted extended canonical human functions and corresponding human data.

C. Extended Canonical Human Function

In [19], it is shown that certain kinematic outputs of human walking can be represented by a single, universal function termed the "canonical human function" — which is the solution to a system of linear spring dampers under constant force. Examination of the data for walking up and down stairs, however, reveals a need for the augmentation of this function. It is found that both walking up and down stairs can be considered as the response of a spring-damper system to a constant force with sinusoidal excitation, which has the form

$$\begin{aligned} y =& e^{-\zeta\omega_n}\left(c_0\cos(\sqrt{1-\zeta^2}\omega_n t) + c_1\sin(\sqrt{1-\zeta^2}\omega_n t)\right) \\ &+ c_2\cos(\omega t) + c_3(\omega_n,\omega,\zeta,c_2)\sin(\omega t) + y_0. \end{aligned} \tag{1}$$

Intuitively, one can consider the constant force as gravity and the sinusoidal excitation is incurred via the elevation change of the impact surface (stairs). Manipulation of (1) yields the following equation, which we term the *extended canonical human function*:

$$\begin{aligned} y_H(t) = e^{-a_1 t}(a_2\cos(a_3 t) + a_4\sin(a_3 t)) + \\ a_5\cos(a_6 t) + \kappa(\alpha)\sin(a_6 t) + a_7. \end{aligned} \tag{2}$$

where $\kappa(\alpha) = (2a_1a_5a_6)/(a_1^2 + a_3^2 - a_6^2)$. In the proceeding subsection, it is shown that the extended canonical human function represents, with high correlation, certain outputs of human locomotion data.

D. Function Fitting

We now seek various constraints of the human data which seem to describe the fundamental outputs of the human locomotion system. A total of four kinematic constraints are required for the 4-DOF robot model in consideration. The constraints which seem to most fully describe the human

locomotion system are: the forward position of the hip,

$$p_{hip} = L_c \sin(-\theta_{sf}) + L_t \sin(-\theta_{sf} - \theta_{sk}),$$

where L_c and L_t are the lengths of the calf and thigh, respectively; the nonstance slope,

$$m_{nsl} = \frac{p^x_{nsf} - p^x_{hip}}{p^z_{nsf} - p^z_{hip}},$$

which defines the slope of a virtual line segment connecting the hip and the non-stance foot; the stance knee θ_{sk}; and the non-stance knee, θ_{nsk}. These constraints are illustrated on the robot model, in Fig. 3(c).

To fit a function to the data, we find the set of parameters a_i which minimizes the error between the function and the data; mathematically, this can be written as an optimization problem

$$\min_{\{a_i\}_{i=1}^7} \sum_{k=1}^{K} (y_d(\tau[k], a_i, \ldots, a_7) - x[k])^2, \tag{3}$$

where $\tau[k]$ and $x[k]$ represent the time and human data, respectively, with $k \in [1, \ldots, K] \subset \mathbb{Z}$ an index for the K data points, and $y_d(\cdot)$ the fitting function with parameters $a_1, \ldots, a_7$. The parameters obtained through this process are given in Table I, together with the correlation of each function to the corresponding set of data. Additionally, the functions for each kinematic constraint and each locomotion behavior are plotted with the corresponding data in Fig. 2. These functions are used in the development of locomotion controllers, as described in section IV.

III. ROBOT MODEL

Naturally, we choose to create a robot based on the human test subject. To reduce computational intensity, while preserving the form of the human lower-body, we construct the model as a serial chain of rigid links. Each link l has a length L_l and a mass m_l, which is a "lumped", or point, mass located a distance r_l from the base of the link. The resulting model configuration is shown in Fig. 3(a), while the mass and length distribution is shown in Fig. 3(b). The specific values of these parameters are obtained by applying

TABLE I: Fitted parameter values for human functions.

$y_1^d = a_1 t, \quad y_2^d = y_H(t)$ given in (2)								
f.	a_1	a_2	a_3	a_4	a_5	a_6	a_7	Corr.
p^{fg}_{hip}	0.921	0	0	0	0	0	0	0.9982
p^{us}_{hip}	0.273	0	0	0	0	0	0	0.9954
p^{ds}_{hip}	0.357	0	0	0	0	0	0	0.9976
m^{fg}_{nsl}	-1.135	0.062	6.495	0.217	0	0	0.150	0.9995
m^{us}_{nsl}	-0.515	0.057	5.515	0.162	0.046	14.864	-0.017	0.9996
m^{ds}_{nsl}	0.475	0.242	6.937	0.149	0.008	23.294	-0.076	0.9999
θ^{fg}_{sk}	2.475	-0.188	10.248	-0.011	0	0	0.358	0.9861
θ^{us}_{sk}	2.013	1.028	3.705	0.639	0.023	14.375	0.514	0.9994
θ^{ds}_{sk}	1.775	-2.383	0.6909	-8.130	-0.130	11.374	2.852	0.9390
θ^{fg}_{nsk}	-0.849	-0.288	9.131	-0.123	0	0	0.593	0.9976
θ^{us}_{nsk}	0.089	-0.850	5.367	-0.161	0.157	14.268	1.046	0.9996
θ^{ds}_{nsk}	-1.222	0.330	6.266	0.312	-0.066	15.422	1.289	0.9999

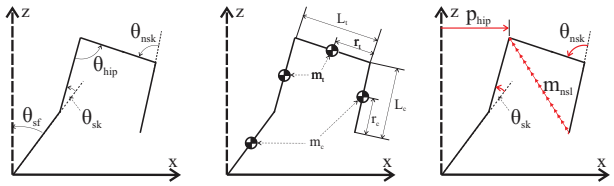

(a) Robot configuration. (b) Robot mass-length. (c) Robot outputs.

Fig. 3: The modeled robot's configuration, mass & length distribution, and virtual constraints.

Winter's [20] mass and length distribution to the human test subject.

Modeling Assumptions As is common in the robotic literature [21], we assume that each leg terminates in a point foot, and the evolution of the biped consists of alternating phases of single and double support. In single support, the support leg, labeled the "stance" leg, is pinned to the ground, while the "non-stance" leg swings freely. Double support phases occur instantaneously and effect a relabeling of the legs, i.e. the previous stance leg becomes the new non-stance leg and vice-versa.

Single Support Dynamics. To obtain the equations of motion for the continuous phase of the robot model, we choose to use the method of Lagrange; specifically, we compute the Lagrangian $\mathcal{L}$ of this system as:

$$\mathcal{L}(q, \dot{q}) = K(q, \dot{q}) - V(q), \tag{4}$$

where $K(q, \dot{q})$ is the kinetic energy and $V(q)$ is the potential energy of the system. The Euler-Lagrange equations,(see [22]), can then be used to obtain the dynamic model:

$$D(q)\ddot{q} + H(q, \dot{q}) = B(q)u \tag{5}$$

with inertia map $D(q)$ and torque distribution map $B(q)$, and

$$H(q, \dot{q}) = C(q, \dot{q})\dot{q} + G(q)$$

containing terms resulting from the Coriolis effect and gravity; $C(q, \dot{q})$ can be found using standard methods [22]. Manipulation of (5) leads to the control system for single support, FG:

$$\dot{x} = f(q, \dot{q}) + g(q)u, \tag{6}$$

where $f(q, \dot{q})$ and $g(q)$ are defined as:

$$f(q, \dot{q}) = \begin{bmatrix} \dot{q} \\ -D^{-1}(q)H(q, \dot{q}) \end{bmatrix}, \; g(q) = \begin{bmatrix} \mathbf{0} \\ D^{-1}(q)B(q) \end{bmatrix}. \tag{7}$$

Double Support Dynamics. As indicated in the modeling assumptions, the double support phase occurs instantaneously; therefore, the dynamic response is modeled as an impact on the system. Specifically, the method of [23] is used, in which plastic rigid-body impacts are modeled as impulse responses. To apply this method, it is necessary to assume that the stance foot is free to move; this requires the augmentation of the configuration space $\mathcal{Q}$ to include the position of the stance foot. Let p be the xz-position of the

stance foot, then the *generalized coordinates* can be written as: $q_e = (p_x, p_z, q) \in \mathcal{Q}_e = \mathbb{R}^2 \times \mathcal{Q}$.

Without loss of generality, we assume that the values of the extended coordinates are zero throughout the gait, i.e. the stance foot is pinned at the origin. Therefore, we introduce the embedding $\iota : \mathcal{Q} \to \mathcal{Q}_e$ defined by $q \mapsto (0, 0, q)$; which associates the generalized coordinates with the shape coordinates.

The impact model [23] under consideration assumes that an impulsive force is applied at the non-stance foot upon impact with the ground. Therefore, let $\Upsilon(q_e)$ be the planar position of the non-stance foot relative to the position of the stance foot, p. Let $J(q_e) = d\Upsilon(q_e)$ be the Jacobian of Υ. The *impact map* gives the post-impact velocity in terms of the pre-impact state:

$$\dot{q}^+ = P(q_e, \dot{q}_e^-) = \\ (I - D^{-1}(q_e)J^T(q_e)(J(q_e)D^{-1}(q_e)J(q_e))^{-1}J(q_e))\dot{q}_e^- \tag{8}$$

with I the identity matrix.

To affect the modeling statement that the legs be "switched" at impact, and thereby reduce the complexity of the model, a coordinate transformation $\mathcal{R}$ (i.e., a *state relabeling procedure*) is introduced. The practice of leg switching is common in bipedal robotic literature [24] and can be implemented in the reset map as follows:

$$\Delta(q, \dot{q}) = \begin{bmatrix} \mathcal{R} & \mathbf{0} \\ \mathbf{0} & \mathcal{R} \end{bmatrix} \begin{bmatrix} \pi \circ \iota(q) \\ \pi^* \circ P(\iota(q), \iota^*(\dot{q})) \end{bmatrix}, \tag{9}$$

where ι^* is the pushforward of ι and π is the canonical projection associated with ι with pushforward π^*. The reset map (9) maps the robot from a double support phase to a single support phase.

IV. Controller Design

The purpose of this section is to specify a controller, u, for the given control system (7). Motivated by the desire to obtain human-like, bipedal robotic locomotion, we seek to construct a controller which drives outputs of the robot to corresponding outputs of the human. Formally, we seek a u which guarantees that $y^a(q) \to y^d(t)$ as $t \to 0$, where y^a is the actual value of the constraint on the robot and y^d is the value of the extended canonical human function. As the dynamics of the robot model are highly nonlinear, the natural choice of control method for this system is Input/Output Linearization [25].

Parameterization of Time. Attracted by the perks of *autonomous* control, we introduce a state-based parameterization of time in our system; this is a common practice in [26], [21]. Examination of human data reveals that the forward position of the hip evolves in an approximately-linear manner with respect to time, that is $p_{hip}(t, v_{hip}) \approx v_{hip}t$, where p_{hip} denotes the forward position of the hip and v_{hip} denotes the forward velocity of the hip. Taking advantage of this observation, the following parameterization of time is formed:

$$\tau(q) = \frac{p_{hip}^R(q) - p_{hip}^R(q^+)}{v_{hip}}. \tag{10}$$

where p_{hip}^R is the forward position of the robot's hip at the beginning of the current step, and v_{hip} is the forward velocity of the human hip, obtained from the locomotion data.

Controller Specification. With the parameterization of time in place, the control law can be formed. The construction of this control law uses the human walking functions considered in Sect. II. In particular, in that section we found that human outputs are described by the human walking functions, or that we can write:

$$\begin{aligned} p_{\text{hip}}^d(t, v_{\text{hip}}) &= v_{\text{hip}}t, & m_{nsl}^d(t, \alpha_{nsl}) &= y_H(t, \alpha_{nsl}), \\ \theta_{sk}^d(t, \alpha_{sk}) &= y_H(t, \alpha_{sk}), & \theta_{nsk}^d(t, \alpha_{nsk}) &= y_H(t, \alpha_{nsk}), \end{aligned} \tag{11}$$

for y_H the canonical walking function in (2) and where, for example, $\alpha_{nsl} \in \mathbb{R}^7$ are the parameters in this equation. Note that all of the parameters can be combined into a single of parameters: $\alpha = (v_{\text{hip}}, \alpha_{nsl}, \alpha_{nsk}, \alpha_{sk}) \in \mathbb{R}^{22}$. With these functions in mind, we define the (relative degree 2) actual outputs of the robot to be the output function considered in Sect. II and the desired outputs to be the outputs of the human as represented by the walking functions:

$$y^{a,2}(q) = \begin{bmatrix} m_{nsl}(q) \\ \theta_{sk} \\ \theta_{nsk} \end{bmatrix}, \; y^{d,2}(t) = \begin{bmatrix} m_{nsl}^d(t, \alpha_{nsl}) \\ \theta_{sk}^d(t, \alpha_{sk}) \\ \theta_{nsk}^d(t, \alpha_{nsk}) \end{bmatrix}. \tag{12}$$

Similarly, with the goal of controlling the velocity of the robot, we define the relative degree 1 outputs to be the velocity of the hip and the desired velocity of the hip:

$$y^{a,1}(q, \dot{q}) = dp_{\text{hip}}(q)\dot{q}, \qquad y^{d,1} = v_{\text{hip}}. \tag{13}$$

The goal is for the outputs of the robot to agree with the outputs of the human, motivating the final form of the outputs to be used in feedback linearization:

$$y_1(q, \dot{q}) = y^{a,1}(q, \dot{q}) - v_{hip}, \tag{14}$$

$$y_2(q, \dot{q}) = y^{a,2}(q, \dot{q}) - y^{d,2}(\tau(q)) \tag{15}$$

As $y_1(q, \dot{q})$ is the forward velocity of the hip, the system has a mixed relative degree. Group the output functions as:

$$y(q, \dot{q}) = (y_1^T(q, \dot{q}), y_2^T(q))^T, \tag{16}$$

where y_1 and y_2 are the relative degree one and two outputs, respectively. The feedback linearization controller, $u(q, \dot{q})$, can now be stated as:

$$u(q, \dot{q}) = -\mathcal{A}^{-1}(q, \dot{q}) \left(\begin{bmatrix} 0 \\ L_f L_f y_2(q) \end{bmatrix} + \begin{bmatrix} L_f y_1(q, \dot{q}) \\ 2\varepsilon L_f y_2(q, \dot{q}) \end{bmatrix} + \begin{bmatrix} 2\varepsilon y_1(q, \dot{q}) \\ \varepsilon^2 y_2(q) \end{bmatrix} \right), \tag{17}$$

with control gain ε and decoupling matrix $A(q)$ given by

$$\mathcal{A}(q, \dot{q}) = \begin{bmatrix} L_g y_1(q, \dot{q}) \\ L_g L_f y_2(q, \dot{q}) \end{bmatrix}$$

The goal of Sect. V will be to determine the parameters, α, of this control law to achieve different walking behaviors based upon the human data.

V. HYBRID AND META-HYBRID SYSTEMS

In this section, it is shown that primary modes of bipedal locomotion - such as walking, running, standing, jumping and traversing stairways - can each be represented by a unique hybrid control system. However, control of functional bipedal robots requires dominion over *multiple* primary modes of locomotion. Therefore, to develop a functional locomotion control scheme, one must introduce auxiliary hybrid systems, which evolve the state of the robot during transitions between primary modes. To this end, we propose the concept of a meta-hybrid system, which consists of both primary and auxiliary hybrid systems.

A. Hybrid Systems

The next step in the modeling process is to develop an abstract mathematical representation of the dynamics of the robot. Given the Lagrangian and impact dynamics of the robot model in Section III, a natural choice of mathematical representation for this model is a hybrid system, or system with impulse effects [24], which exhibits both continuous and discrete dynamics.

Definition 1: A *hybrid control system* is a tuple,

$$\mathscr{HC} = (\mathcal{D}, S, \Delta, f, g, U),$$

where

- $\mathcal{D}$ is the *domain* with $\mathcal{D} \subseteq \mathcal{X}$ a smooth submanifold of the state space $\mathcal{X} \subseteq \mathbb{R}^n$,
- $S \subset \mathcal{D}$ is a proper subset of $\mathcal{D}$ called the *guard* or *switching surface*,
- $\Delta : S \to \mathcal{D}$ is a smooth map called the *reset map*,
- (f, g) is a *control system* on $\mathcal{D}$, i.e., $\dot{x} = f(x) + g(x)u$,
- $U \subseteq \mathbb{R}^m$ is the set of admissible control.

A *hybrid system* is a hybrid control system with $U = \emptyset$, e.g., any applicable feedback controllers have been applied, making the system closed-loop. In this case,

$$\mathscr{H} = (\mathcal{D}, S, \Delta, f),$$

where f is a *dynamical system* on $\mathcal{D} \subseteq \mathcal{X}$, i.e., $\dot{x} = f(x)$.

Hybrid Period Orbits and the Poincaré Map. In order to establish the stability of k-periodic orbits, we will use the standard technique of studying the corresponding Poincaré map. In particular, taking G to be the Poincaré section, one obtains the Poincaré map, $P : G \to G$, which is a partial map defined by:

$$P(z) = c(\tau(z)).$$

where $c(t)$ is the solution to $\dot{x} = f(x)$ with $c(0) = R(z)$ and $\tau(z)$ is the *time-to-impact* function. In particular, if z^* is a k-fixed point of P (under suitable assumptions on z^*, G, and the transversality of $\mathcal{O}$ and G) a k-periodic orbit $\mathcal{O}$ with $z^* \in \mathcal{O}$ is locally exponentially stable if and only if P^k is locally exponentially stable (as a discrete-time dynamical system, $z_{i+1} = P(z_i)$). Although it is not possible to explicitly compute the Poincaré map, one can compute a numerical approximation of this map through simulation and thereby test its stability numerically. This gives a concrete method for practically testing the stability of periodic orbits.

Hybrid System for the Biped. Given the preceeding definitions, we can now build a hybrid system representation of the robot model of this study. Formally, we begin by writing the hybrid control system for the robot as:

$$\mathscr{HC}_h^R = (\mathcal{D}_h^R, S_h^R, \Delta^R, f^R, g^R, U^R), \tag{18}$$

which depends on a unilateral constraint function, h, that represents the environment, or *terrain* of the hybrid system. Specifically, h is the height of non-stance foot above the walking surface, e.g. a staircase or flat ground; h characterizes the allowable configuration, i.e. the domain, which is given by:

$$\mathcal{D}_h^R = \{(q, \dot{q}) \in T\mathcal{Q} : h(q) \geq 0\}. \tag{19}$$

The guard is just the boundary of the domain with the additional assumption that the unilateral constraint is decreasing, i.e., the vector field is pointed outside of the domain, or

$$S_h^R = \left\{(q, \dot{q}) \in T\mathcal{Q} : h(q) = 0 \text{ and } \frac{\partial h(q)}{\partial q}\,\dot{q} < 0\right\}. \tag{20}$$

The remaining elements are specified by the dynamics of the robot; that is, they are intrinsic to the model and consistent for all hybrid system representations of the robot, yet they are independent of the terrain. These elements are given by

- Δ^R is the reset map — corresponding to the (*impact equations*) in the double support phase — as defined in (9),
- (f^R, g^R) is a *control system* on $\mathcal{D}^R$ — which governs the evolution of the single support phase — as defined in (7).
- $U^R = \mathbb{R}^4$, as we assume full control authority.

For the hybrid control system $\mathscr{HC}_h^R$, we apply the human-inspired control law (17) to obtain a hybrid system:

$$\mathscr{H}_{(h,\alpha)}^R = (\mathcal{D}_h^R, S_h^R, \Delta^R, f_\alpha^R), \tag{21}$$

with

$$f_\alpha^R(q, \dot{q}) = f^R(q, \dot{q}) + g^R(q, \dot{q})u(q, \dot{q}).$$

Here, we have made the dependence of f_α^R on the parameters $\alpha \in \mathbb{R}^{22}$ of the human walking functions explicit (note that f^R also depends on the control gain ϵ, but since the same gain will be used in all cases for the robot it is not explicitly stated). The end result of the modeling process is a hybrid system $\mathscr{H}_{(h,\alpha)}^R$ that depends on both the terrain it is walking in (through h) and the parameters of the human inspired control α.

B. Meta-Hybrid Systems.

A meta-hybrid system is a hybrid system of hybrid systems, which contains multiple locomotion behaviors and transitions between these behaviors.

Definition 2: A *meta-hybrid system* is a tuple,

$$\mathscr{MH} = (\Gamma, \mathscr{M}, \mathscr{T})$$

where

- $\Gamma = (V, E)$ is a directed graph, with V a set of vertices, or nodes, and $E \subset Q \times Q$ a set of edges; for $e = (q, q') \in E$, denote the source of e by $\mathrm{sor}(e) = q$ and the target of e by $\mathrm{tar}(e) = q'$.
- $\{\mathscr{M}_v\}_{v \in V}$ is a collection of *motion primitives*, each represented by a hybrid system:

$$\mathscr{M}_v = (\mathcal{D}_v, S_v, \Delta_v, f_v, U_v).$$

- $\{\mathscr{T}_e\}_{e \in E}$ is a collection of *motion transitions*, represented by hybrid systems of the form:

$$\mathscr{T}_e = (\mathcal{D}_{\mathrm{tar}(e)}, S_{\mathrm{tar}(e)}, \Delta_{\mathrm{tar}(e)}, f_e).$$

  That is, $\mathscr{T}_e$ has the same domain, guard and reset map as $\mathscr{M}_{\mathrm{tar}(e)}$, but has a different vector field f_e.

It is important to note that the meta-hybrid system of a hybrid system, except that we have placed explicit restrictions on the structure of this system so as to be applicable to bipedal robots that switch between different walking behavior. In particular, as will be seen, we will construct three motion primitives and transitions behaviors to form a meta-hybrid system as illustrated in Fig. 4.

VI. MOTION PRIMITIVES & TRANSITIONS

In this section, we will explicitly construct a meta-hybrid system for a bipedal robot, with the motion primitives—walking on flat ground, walking upstairs and walking downstairs—and transitions between these behaviors. The behavior of the robot performing these transitions and motion primitives will be supported through simulation results. More formally, the goal of this section is to construct a meta-hybrid system for the bipedal robot:

$$\mathscr{M}\mathscr{H}^R = (\Gamma^R, \mathscr{M}^R, \mathscr{T}^R).$$

Since the three motion primitives we are interested in are walking on flat ground, walking up stairs, and walking down stairs, we have the directed graph $\Gamma^R = (V^R, E^R)$, where

$$\begin{aligned} V^R &= \{fg, us, ds\} \\ E^R &= \{(fg, us), (us, fg), (fg, ds), (ds, fg)\} \end{aligned}$$

or we allow transitions between walking on flat ground and going up and down stairs (but not transitions between going up stairs and going down stairs). The graph Γ^R can be seen in Fig. 4. The remainder of this section will be devoted to constructing the motion primitives and motion transitions.

A. Motion Primitives

Motion primitives are the core modes of locomotion of this study; this section discusses the development of controllers for motion primitives and the simulations resulting from the application of these controllers to the robot model.

Motion Primitive Collection. Using the concepts developed throughout this paper, and specifically Sect. IV, we can now construct mathematical representations a bipedal robot traversing each of the three different terrains of interest: walking on flat ground fg, up stairs us, and down stairs ds. In particular, for each of the three terrains we obtain a hybrid system (of the form given (21)) modeling the biped in this terrain:

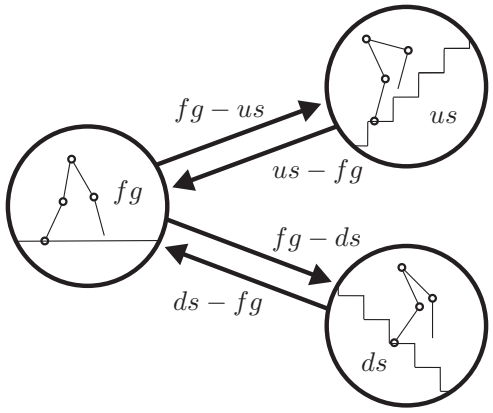

Fig. 4: Graph of a meta-system representation for the three motion primitives in consideration.

- *Flat Ground:* $\mathscr{H}^R_{(h_{fg}, \alpha_{fg})}$, where $h_{fg}(q) = z_{nsf}(q)$ is the height of the foot above flat ground,
- *Up Stairs:* $\mathscr{H}^R_{(h_{us}, \alpha_{us})}$, where $h_{us}(q) = z_{nsf}(q) - z_{stair}$ is the height of the foot above a stair (with the stair above the stance foot).
- *Down Stairs:* $\mathscr{H}^R_{(h_{ds}, \alpha_{ds})}$, where $h_{ds}(q) = z_{nsf}(q) + z_{stair}$ is the height of the foot above a stair (with the stair below the stance foot).

To achieve motion primitives from these hybrid systems, it is necessary to design controllers for each motion primitive, i.e., determine the control parameters α_v, $v \in V^R$, that will result in stable walking for the robot in each terrain.

Controller Development. To obtain the control parameters α_v, $v \in V^R$, for each motion primative, we use the method of [15] which uses human data in the form of an optimization subject to constraints that imply stable walking. In particular, we solve the optimization problem (22) of [15]:

$$\begin{aligned} \alpha_v^* = \underset{\alpha \in \mathbb{R}^{22}}{\mathrm{argmin}} \ & \mathrm{Cost}^v_{\mathrm{HD}}(\alpha) \\ \text{s.t.} \ & \Delta^R(S^R_{h_v} \cap \mathbf{Z}_\alpha) \subset \mathbf{PZ}_\alpha \end{aligned} \tag{22}$$

where $\mathrm{Cost}^v_{\mathrm{HD}}$ is the human-data-based cost function, (11) of [15], which is the weighted-sum of squared errors between the output functions and corresponding data; note that since this cost depends on the human data, it is indexed by $v \in V^R$ since for each motion primitive one obtains a different cost. Moreover, the constraints of the optimization depend on the constraint function h_v, $v \in V^R$, i.e., they depend on the specific terrain being considered. Finally, $\mathbf{Z}_\alpha$ is a *zero dynamics surface* of the system, on which $y^{a,1}(q, \dot{q}) = y^{d,1}$ and $y^{a,2}(q) = y^{d,2}(q)$ for all time; $\mathbf{PZ}_\alpha$ is a *partial zero dynamics surface* of the system, on which $y^{a,2}(q) = y^{d,2}(q)$ for all time. Due to space constraints, we refer the reader to [15] for further details.

By solving the optimization problem (22) for each motion primitive, we obtain control parameters α_v^*, $v \in V^R$ that yield stable walking behavior for each motion primitive (this

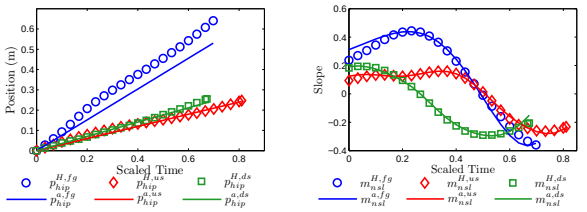

(a) Optimized hip velocity (b) Optimized nonstance slope

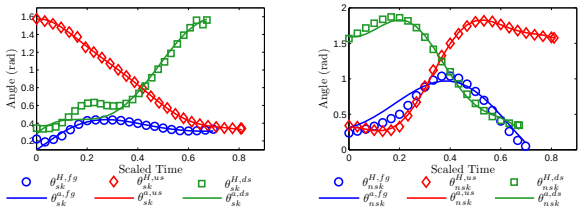

(c) Optimized stance knee angle (d) Optimized nonstance knee angle

Fig. 5: Optimized extended canonical human functions with parameters obtained by solving the optimization problem (22) and the corresponding human data.

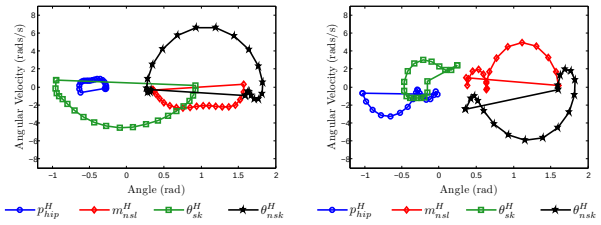

(a) Periodic orbit for $\mathscr{M}_{as}$. (b) Periodic orbit for $\mathscr{M}_{ds}$.

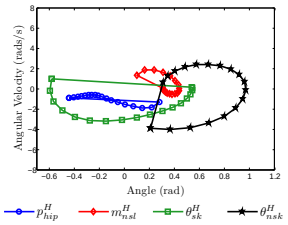

(c) Periodic orbit for $\mathscr{M}_{fg}$.

Fig. 6: Phase portraits for the motion primitives.

will be justified through simulation in the next paragraph). That is, we have thus obtained the motion primitives for $\mathscr{M}\mathscr{H}^R$ given by $\mathscr{M}_v^R = \mathscr{H}^R_{(v,\alpha^*_{h_v})}$, $v \in V^R$. Plotting the human walking functions with the specific parameters α_v^* found by solving this optimization problem, as compared against the human data, can be seen in Fig. 5. By inspecting that figure, it can be seen that the canonical human walking functions that yield walking for each motion primitive have very good agreement with the human walking data.

Simulations. A simulation for each motion primitive was performed. The resulting locomotion gaits from simulation are given in Fig. 7; these figures show the evolution of the robot during the single support phase of the gait, each of

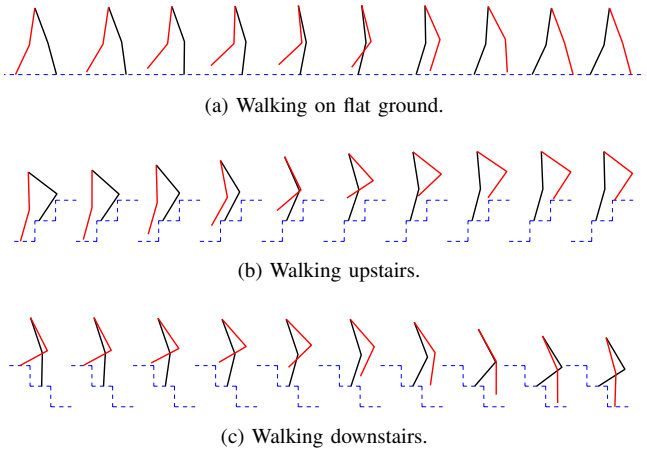

(a) Walking on flat ground.

(b) Walking upstairs.

(c) Walking downstairs.

Fig. 7: Snapshots from robotic locomotion simulations exhibiting the three motion primitives.

which qualitatively resembles the corresponding human gait quite well. The phase portraits for each motion primitive simulation are shown in Fig 6. Numerical approximations of the Poincaré map yield eigenvalues which are all less than one, which implies the corresponding motion primitives are stable.

B. Motion Transitions

This section discusses the development and simulation of motion transitions, which are explicitly built upon the motion primitives obtained in the previous section.

Motion Transition Collection. We are interested in developing motion primitives based upon the meta-hybrid system graph Γ^R, which gives the allowable transitions between different walking behaviors. Based upon the definition of a mete-hybrid systems (Definition 2), the motion transitions must satisfy very specific conditions with regard to the motion primitives. Therefore, specific motion transition hybrid systems we are interested in must have the form:

- *Walking on flat ground to up stairs:* $\mathscr{H}^R_{(h_{us},\alpha_{(fg,us)})}$
- *Walking up stairs to flat ground:* $\mathscr{H}^R_{(h_{fg},\alpha_{(us,fg)})}$
- *Walking on flat ground to down stairs:* $\mathscr{H}^R_{(h_{ds},\alpha_{(fg,ds)})}$
- *Walking down stairs to flat ground:* $\mathscr{H}^R_{(h_{fg},\alpha_{(ds,fg)})}$

Therefore, to define the transition behaviors, it is necessary to determine the control parameters α_e, $e \in E$. This will be achieved through another optimization, but one that uses the walking behavior of the motion primitives to smoothly transition from one behavior to another.

Controller Development. To determine the parameters α_e, $e \in E$, of the motion transitions we use the fixed points corresponding to the stable walking of each motion primitive. In particular, let $(q_v^*, \dot{q}_v^*) \in S^R_{h_v}$, $v \in V^R$, be the fixed point of each motion primitive; this is the unique point on the periodic orbit that intersects the guard. Using this, and at a high level, the goal of the motion transition optimization is to generate desired output functions, which have smooth connections with the corresponding source and the target

motion primitives. Formally, these objectives can be stated in an optimization problem:

$$\begin{aligned} \alpha_e^* = \underset{\alpha\in\mathbb{R}^{22}}{\operatorname{argmin}} \; & \dot{y}^{d,2}_{\alpha_e}(\tau(q^*_{\mathrm{tar}(e)})) \\ \text{s.t} \quad & y^{d,2}_{\alpha_e}(0) - y^{d,2}_{\alpha^*_{sor(e)}}(0) = 0 \\ & \dot{y}^{d,2}_{\alpha_e}(0) - \dot{y}^{d,2}_{\alpha^*_{sor(e)}}(0) = 0 \\ & y^{d,2}_{\alpha_e}(q^-) - y^{d,2}_{\alpha^*_{tar(e)}}(\tau(q^*_{\mathrm{tar}(e)})) = 0 \end{aligned} \tag{23}$$

where here, $y^{d,2}_{\alpha}(t)$ is the desired output of the robot consisting of the human walking functions (12) (where we have made the dependence of this function on the parameters α explicit), $\alpha^*_{\mathrm{tar}(e)}$ are the parameters of the motion primitive $\mathscr{M}^R_{\mathrm{tar}(e)}$ obtained by solving the optimization problem (22), $(q^*_{\mathrm{tar}(e)}, \dot{q}^*_{\mathrm{tar}(e)})$ is the fixed point of the periodic orbit for this motion primitive, and τ is the parameterization of time in (10). Solving this optimization problem yields parameters α^*_e, $e \in E^R$, and we thus obtained our motion transition hybrid systems: $\mathscr{T}_e = \mathscr{H}^R_{(h_{\mathrm{tar}(e)},\alpha^*_e)}$ with $e \in E^R$.

Simulations. Three simulations were performed in which motion primitves and motion transitions were combined. To construct a Poincaré map, and thus establish a notion of the stability of a meta-system, the biped must start and end in the same mode; therefore, we chose to simulate two locomotion cycles: walking on flat ground to walking up stairs to walking on flat ground (F-US-F) and walking on flat ground to walking down stairs to walking on flat ground (F-DS-F). Numerical approximation yields eigenvalues for both simulations; the maximum eigenvalue of each is below unity which implies that both meta-systems are stable. Finally, we simulated all three motion primitives together with the four motion transitions; snapshots from the simulation can be seen in Fig. 8.

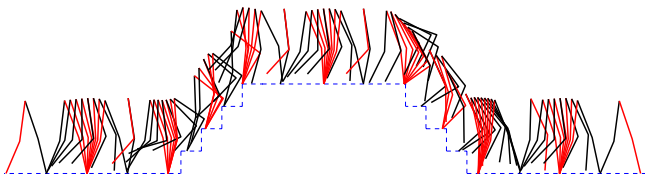

Fig. 8: Snapshots from the simulated composition of multiple locomotion modes.

VII. CONCLUDING REMARKS

In this paper, we examined experimental human data on three modes of walking. It is shown that certain outputs of the flat ground *and* stair-climbing data can each be represented by the response of a linear spring-damper system. An optimization of the parameters in (2) gives virtual outputs for feedback liberalization controllers; implementation of these controllers yields stable, periodic locomotion in simulation.

A second optimization yields controllers which effect transitions between motion primitives; these intermediate modes are termed *motion transitions*. Simulations are given which display bipedal robots walking in a varying terrain. A future project will be to expand the set of motion primitives to additional locomotion behaviors.

REFERENCES

[1] S. Collins, A. Ruina, R. Tedrake, and M. Wisse, "Efficient bipedal robots based on passive-dynamic walkers," *Science*, vol. 307, pp. 1082–1085, Feb. 2005.

[2] M. W. Spong and F. Bullo, "Controlled symmetries and passive walking," *IEEE TAC*, vol. 50, no. 7, pp. 1025–1031, 2005.

[3] T. McGeer, "Passive dynamic walking," *Intl. J. of Robotics Research*, vol. 9, no. 2, pp. 62–82, Apr. 1990.

[4] C. Chevallereau, D. Djoudi, and J. W. Grizzle, "Stable bipedal walking with foot rotation through direct regulation of the zero moment point," *IEEE TRO*, vol. 25, no. 2, pp. 390–401, Apr. 2008.

[5] J. Pratt, P. Dilworth, and G. Pratt, "Virtual model control of a bipedal walking robot," in *IEEE Conf. on Robotics and Automation*, Albuquerque, Apr. 1997, pp. 193–198.

[6] N. Fatehi, A. Akbarimajd, and M. Asadpour, "Zmp analysis for dynamic walking of a passivity-based biped robot with flat feet," in *Intl. Conf. on Control Automation and Systems*, Gyeonggi-do, Oct. 2010.

[7] J. Z. B. C. Q. Wang, Y. Huang and L. Wang, "Dynamic walking on uneven terrains with passivity-based bipedal robot," vol. 85, no. 3, pp. 187–199, 2011.

[8] P. S.-H. Z. Qiu-Bo and G. Chao, "Motion planning for humanoid robot based on hybrid evolutionary algorith," vol. 7, no. 3, pp. 209–216, 2010.

[9] http://www.aldebaran-robotics.com/.

[10] H. B. S. P. Brugger, "Simulating prosthetic gait - lessons to learn," vol. 3, no. 1, p. 64, 2003.

[11] D. C. J. K. Rai, R. P.Tewari, "Hybrid control strategy for robotic leg prosthesis using artificial gait synthesis," vol. 1, no. 1, pp. 44–50, 2009.

[12] K. M. Ono, Kyosuke, "Analytical study of active prosthetic legs," vol. 1, no. 3, pp. 548–557, Mar. 2007.

[13] H. Kazerooni, J. L. Racine, L. Huang, and R. Steger, "the control of the berkeley lower extremity exoskeleton," in *Proceedings of the 2005 IEEE International Conference on Robotics and Automation*, Barcelona, Apr. 2005, pp. 4353 – 4360.

[14] J. Rose and J. G. Gamble, *Human Walking*. Philadelphia: Lippincott Williams & Wilkins, Dec. 2005.

[15] A. D. Ames, "First steps toward automatically generating bipedal robotic walking from human data," in *8th International Workshop on Robotic Motion and Control, RoMoCo'11*, Bukowy Dworek, 2011.

[16] http://www.phasespace.com/.

[17] H. W.-H. Lee Yung-Hui, "Effects of shoe inserts and heel height on foot pressure, impact force, and perceived comfort during walking," vol. 36, no. 3, pp. 355–362, May 2005.

[18] D. R. C. D. Frédéric Dierick, Massimo Penta, "A force measuring treadmill in clinical gait analysis," vol. 20, no. 3, pp. 299–303, Dec. 2004.

[19] R. W. Sinnet, M. J. Powell, S. Jiang, and A. D. Ames, "Compass gait revisited: A human data perspective with extensions to three dimensions," in *50th IEEE Conference on Decision and Control and European Control Conference.*, Orlando, Dec. 2011.

[20] D. A. Winter, *Biomechanics and Motor Control of Human Movement*, 2nd ed. New York: Wiley-Interscience, May 1990.

[21] E. R. Westervelt, J. W. Grizzle, C. Chevallereau, J. H. Choi, and B. Morris, *Feedback Control of Dynamic Bipedal Robot Locomotion*. Boca Raton: CRC Press, Jun. 2007.

[22] R. M. Murray, Z. Li, and S. S. Sastry, *A Mathematical Introduction to Robotic Manipulation*. Boca Raton: CRC Press, Mar. 1994.

[23] Y. Hürmüzlü and D. B. Marghitu, "Rigid body collions of planar kinematic chains with multiple contact points," *Intl. J. of Robotics Research*, vol. 13, no. 1, pp. 82–92, Feb. 1994.

[24] J. W. Grizzle, G. Abba, and F. Plestan, "Asymptotically stable walking for biped robots: Analysis via systems with impulse effects," *IEEE TAC*, vol. 46, no. 1, pp. 51–64, Jan. 2001.

[25] S. S. Sastry, *Nonlinear Systems: Analysis, Stability and Control*. New York: Springer, Jun. 1999.

[26] E. R. Westervelt, J. W. Grizzle, and D. E. Koditschek, "Hybrid zero dynamics of planar biped walkers," *IEEE TAC*, vol. 48, no. 1, pp. 42–56, Jan. 2003.